

# A transferable nonorthogonal tight-binding model of germanium: application to small clusters

Jijun Zhao <sup>\*</sup>

*Department of Physics and Astronomy, University of North Carolina at Chapel Hill, Chapel Hill,  
NC 27599, USA.*

*International Centre for Theoretical Physics, P.O.Box 586, Trieste 34100, Italy*

Jinlan Wang, Guanghou Wang

*National Laboratory of Solid State Microstructures, Nanjing University, Nanjing 210093, P.R.  
China*

(October 29, 2018)

## Abstract

We have developed a transferable nonorthogonal tight-binding total energy model for germanium and use it to study small clusters. The cohesive energy, bulk modulus, elastic constants of bulk germanium can be described by this model to considerably good extent. The calculated bulk phase diagram for germanium agrees well with LDA results. The geometries and binding energies found for small  $\text{Ge}_n$  clusters with  $n = 3 - 10$  are very close to previous *ab initio* calculations and experiments. All these results suggest that this model can be further applied to the simulation of germanium cluster of larger size or with longer time scale, for which *ab initio* methods is much more computational expensive.

36.40.Mr, 61.46.+w, 71.15.Fv, 31.15.Rh

Typeset using REVTeX

In the past decade, tight-binding molecular dynamics (TBMD) has evolved into a powerful approach in the simulation of semiconductor materials<sup>1–3</sup>. In the tight-binding scheme, although the system is still described in a quantum-mechanical manner, the computational cost is significantly reduced due to the parameterization of Hamiltonian matrix elements. In many cases of material simulations, it might offer a satisfactory compromise between empirical<sup>4</sup> and first principle<sup>5,6</sup> methods for modeling the interatomic interaction. As an alternative of the accurate but costly *ab initio* molecular dynamics, TBMD can handle more complicated systems with acceptable accuracy<sup>1–3</sup>.

For carbon and silicon, there are several well established orthogonal<sup>7–9</sup> and nonorthogonal<sup>10–12</sup> tight-binding models. Although the orthogonal models works well for various bulk systems<sup>1–3</sup>, Menon found that the inclusion of the nonorthogonality of tight-binding basis is essential for describing the geometries and binding energies of small silicon clusters<sup>11,12</sup>. Compared to carbon and silicon, there is much fewer tight-binding models developed for germanium. Recently, M.Menon has extended the nonorthogonal tight-binding (NTB) scheme to germanium and calculated the structures and cohesive energies of small  $\text{Ge}_n$  clusters<sup>13</sup>. Although the cluster geometries obtained in Ref.[13] are generally consistent with *ab initio* results, the binding energies are overestimated. In this work, we perform an independent fitting of NTB parameters for germanium, which describes binding energies of germanium clusters better than that in Ref.[13]. This model is employed to study some bulk properties and considerably good results are obtained.

In Menon's NTB model<sup>11–13</sup>, the total binding energy  $E_b$  of a system with  $N_a$  atoms can be written as a sum

$$E_b = E_{el} + E_{rep} + N_a E_0 \quad (1)$$

$E_{el}$  is the electronic band energy, defined as the sum of one-electron energies  $\epsilon_k$  for the occupied states:  $E_{el} = \sum_k^{occ} \epsilon_k$ . In Eq.(1), a constant energy correction term  $N_a E_0$  and a repulsive interaction  $E_{rep}$  are also included.

On nonorthogonal basis set, the eigenvalues  $\epsilon_k$  of system are determined from the secular

equation:

$$\det|H_{ij} - \epsilon S_{ij}| = 0. \quad (2)$$

Here the overlap matrix elements  $S_{ij}$  are constructed in the spirit of extended Hückel theory<sup>14</sup>,

$$S_{ij} = \frac{2V_{ij}}{K(\epsilon_i + \epsilon_j)} \quad (3)$$

and the nonorthogonal Hamiltonian matrix elements by

$$H_{ij} = V_{ij} \left[ 1 + \frac{1}{K} - S_2^2 \right] \quad (4)$$

where

$$S_2 = \frac{(S_{ss\sigma} - 2\sqrt{3}S_{sp\sigma} - 3S_{pp\sigma} + 3S_{pp\pi})}{4} \quad (5)$$

is the nonorthogonality between two  $sp^3$  bonding orbitals and  $K$  is a environment dependent empirical parameter<sup>11</sup>.

The  $H_{ij}$  and  $S_{ij}$  depend on the interatomic distance through the universal parameters  $V_{ij}$ , which are calculated within Slater-Koster's scheme<sup>15</sup>. The scaling of the Slater-Koster parameters  $V_{\lambda\lambda'\mu}$  is taken to be exponential with the interatomic distance  $r$

$$V_{\lambda\lambda'\mu}(r) = V_{\lambda\lambda'\mu}(d_0) e^{-\alpha(r-d_0)} \quad (6)$$

where  $d_0 = 2.45\text{\AA}$  is the bond length for germanium crystal in the diamond structure<sup>16</sup>.

The repulsive energy  $E_{rep}$  in Eq.(1) is given by the summation of pairwise potential function  $\chi(r)$ :

$$E_{rep} = \sum_i \sum_{j>i} \chi(r_{ij}) = \sum_i \sum_{j>i} \chi_0 e^{-4\alpha(r_{ij}-d_0)} \quad (7)$$

where  $r_{ij}$  is the separation between atom  $i$  and  $j$ .

In practice, we adopt the Slater-Koster hopping integrals  $V_{\lambda\lambda'\mu}(d_0)$  fitted from the band structure of bulk germanium<sup>17</sup>. The on-site orbital energies  $\epsilon_s$ ,  $\epsilon_p$  are taken from atomic

calculations<sup>18</sup>. The only four adjustable parameters  $\alpha$ ,  $K$ ,  $\chi_0$ ,  $E_0$  are fitted to reproduce the fundamental properties of germanium bulk and dimer. The input properties include: the experimental values of bulk interatomic distance 2.45 Å<sup>16</sup>, dissociation energy 2.65 eV<sup>19</sup> and vibrational frequency (286±5 cm<sup>-1</sup>)<sup>20</sup> of Ge<sub>2</sub> dimer, as well as theoretical bond length of Ge<sub>2</sub> (2.375 Å) from accurate quantum chemistry calculation at G2(MP2) level<sup>21</sup>. The fitted parameters are given in Table I.

## TABLES

Table I. Parameters in the NTB mode developed for germanium in this work. See text for detailed descriptions.

$\epsilon_s$	$\epsilon_p$	$V_{ss\sigma}$	$V_{sp\sigma}$	$V_{pp\sigma}$	$V_{pp\pi}$
-14.38 eV	-6.36 eV	-1.86 eV	1.90 eV	2.79 eV	-0.93 eV
$d_0$	$K$	$\chi_0$	$\alpha$	$E_0$	
2.45 Å	1.42	0.025 eV	1.748 Å <sup>-1</sup>	0.79 eV	

We can first check the validity of the present NTB scheme by studying the fundamental properties of germanium solid in diamond phase. The obtained cohesive energy 3.58 eV/atom is very close to experimental value 3.85 eV/atom<sup>16</sup>. Furthermore, we have calculated the bulk modulus  $B$  and elastic constants  $C_{11}$ ,  $C_{12}$ ,  $C_{44}$  of germanium and compared with experimental values<sup>22</sup> in Table II. Most of the bulk elastic properties such as  $B$ ,  $C_{11}$ ,  $C_{12}$  are well reproduced except that the  $C_{44}$  is overestimated by 0.35 Mbar in our model.

Table II. Bulk modulus and elastic constants (in units of Mbar) of bulk germanium in diamond structure. NTB are the theoretical results from present NTB model; Exper. denote the experimental values taken from Ref.[22].

	$C_{11}$	$C_{12}$	$C_{44}$	$B$
NTB	1.125	0.545	1.019	0.738
Exper.	1.288	0.483	0.671	0.751

## FIGURES

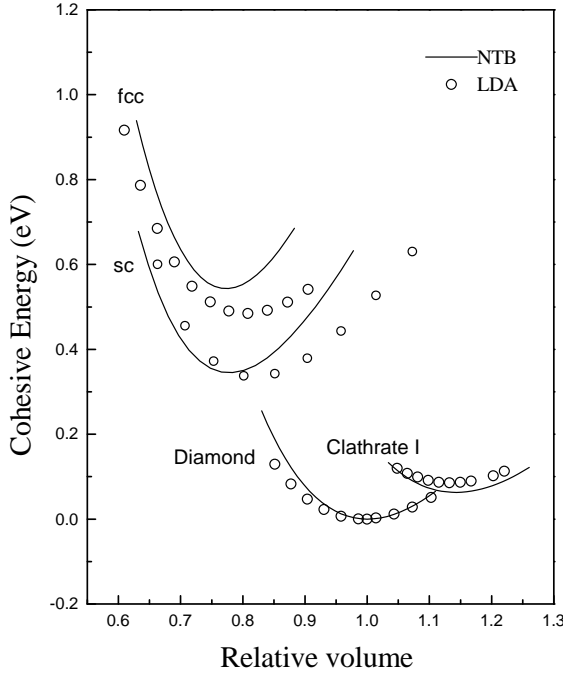


FIG. 1. Cohesive energies vs. relative volume for bulk germanium in simple cubic (sc), diamond and clathrate I phase from NTB (solid line) and LDA (open circle) calculations<sup>23</sup>.

By using the NTB scheme, we have also calculated the equation of states of germanium in different phases. In Fig.1, we present the zero-temperature phase diagram of the fcc, sc, diamond and type I clathrate obtained from NTB model, along with recent LDA plane-wave pseudopotential calculations<sup>23</sup>. It is worthy to noted that our NTB model is able to described the energy and atomic volume of clathrate phase. The energy of clathrate I is 0.06 eV/atom higher than that of diamond phase and its relative volume is about 15% larger than diamond phase. These results are consistent with the 0.08 eV energy difference and 15% volume change from LDA calculation<sup>23</sup>. The success in clathrate phase is important since the clathrate is also four-coordinated structure<sup>23</sup>. On the other hand, it is natural to find that the agreement between LDA and NTB scheme become worse in the high-coordinated phases like fcc since the present model is fitted from the diamond phase and dimer. However, the relative poor description of high coordinate phase will not influence the study on germanium

clusters since such high coordination ( $\sim 12$ ) does not exist in the geometries of germanium clusters. Considering its extreme simplicity and small number of adjustable parameters, the current NTB scheme gives a sufficient satisfactory overall description of bulk germanium properties. Therefore, one can expect that the model to give a reasonable description on the germanium clusters.

In this paper, we determine the lowest energy structures of the  $\text{Ge}_n$  clusters with  $n = 3 - 10$  by using TBMD full relaxation. The ground state structures of  $\text{Ge}_n$  ( $n = 5 - 10$ ) are presented in Fig.2 and the geometrical parameters of small  $\text{Ge}_n$  ( $n = 3 - 7$ ) clusters are compared with previous *ab initio* calculations<sup>24-27</sup> in Table III. In general, both the lowest energy structures and their characteristic bond length agree well with *ab initio* results. A brief description is given in the following.

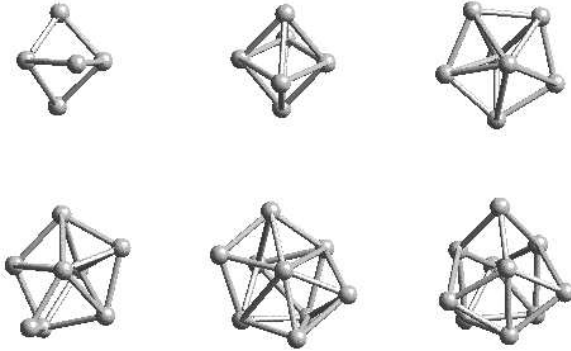


FIG. 2. Lowest energy structures of  $\text{Ge}_n$  ( $n = 5 - 10$ ) clusters.

Table III. Lowest energy geometries (with characteristic bond length parameters) of small  $\text{Ge}_n$  clusters. Tight-binding calculation (NTB) are compared with previous *ab initio* results such as: MRSDCI<sup>24</sup>, B3LYP<sup>25</sup>, LDA<sup>26,27</sup>. The label of atom and bond for  $\text{Ge}_n$  are taken from Ref.29.

$n$	Sym.	Bond	Bond length (Å)				
			MRSDCI <sup>24</sup>	B3LYP <sup>25</sup>	LDA <sup>26</sup>	LDA <sup>27</sup>	NTB
3	$C_{2v}$	1-2	3.084	3.070	3.20	2.91	2.71

		1-3	2.320	2.312	2.26	2.21	2.38
4	$D_{2h}$	1-2	2.477	2.475	2.40	2.35	2.44
		1-3	2.622	2.619	2.53	2.44	2.57
5	$D_{3h}$	1-2	3.277	3.135	3.19	3.10	2.87
		1-3	2.456	2.476	2.39	2.34	2.44
		3-4	2.456	3.320	3.19	3.10	3.40
6	$O_h$	1-2	—	2.553	2.47	2.40	2.47
		2-3	—	2.941	2.85	2.78	2.70
7	$D_{5h}$	1-2	—	—	2.65	2.56	2.83
		1-3	—	—	2.57	2.49	2.57
		3-4	—	—	2.59	2.51	2.53

The minimum energy structure found for  $\text{Ge}_3$  is an isosceles triangle ( $\text{C}_{2v}$ ) with bond length 2.38 Å and apex angle  $\theta = 69.5^\circ$ , in agreement with *ab initio* calculations (see Table III for comparison). The linear chain has higher total energy of about 0.95 eV.

The ground state structure of germanium tetramer is a planar rhombus ( $\text{D}_{2h}$ ) with side length 2.44 Å and minor diagonal length 2.57 Å. This structure has been predicted as ground state in all *ab initio* calculations<sup>21,24–28</sup> and the tight-binding bond length are close to *ab initio* results.

For the  $\text{Ge}_5$ , the lowest energy configuration is obtained as a strongly compressed trigonal bipyramidal ( $\text{D}_{3h}$ ). The energy of structure is lower than the perfect trigonal bipyramidal by 0.62 eV and the planar edge capped rhombus by 0.35 eV. The trigonal bipyramidal structure has been considered in all of the previous *ab initio* studies<sup>21,24–28</sup>. In those LDA based simulation without symmetry constraint<sup>25,26,28</sup>, the trigonal bipyramidal is found to undergo severe compression and relax to the structure in Fig.2.

A distorted octahedron ( $\text{D}_{4h}$ ) is obtained for  $\text{Ge}_6$  as lowest energy structure. This structure is found to be energetically degenerated with a edge-capped trigonal bipyramidal ( $\Delta E = 0.018$  eV). This result agree well with recent B3LYP and Car-Parrinello calculation of  $\text{Ge}_6$ <sup>27,28</sup>.

In the case of  $\text{Ge}_7$ , we find a compressed pentagonal bipyramidal with  $\text{D}_{5h}$  symmetry as ground state and energetically lower than the face capped octahedron by 0.63 eV. The pentagonal bipyramidal structure has also been obtained from LDA based simulations<sup>25,26,28</sup>.

Table IV. Binding energy per atom  $E_b/n$  (eV) of  $\text{Ge}_n$  clusters obtained within the present NTB model, compared to experimental values<sup>19,30</sup>, *ab initio* results based on G2(MP2) level<sup>21</sup> or LDA plane-wave pseudopential<sup>26,28</sup>, as well as nonorthogonal tight-binding<sup>13</sup> calculations.

$n$	Exper. <sup>19,30</sup>	G2(MP2) <sup>21</sup>	LDA <sup>26</sup>	LDA <sup>27</sup>	NTB <sup>13</sup>	NTB(present)
2	1.32	1.25	1.89	–	1.31	1.32
3	2.24	2.02	2.78	2.66	2.11	2.06

4	2.60	2.49	3.32	3.19	2.66	2.62
5	2.79	2.68	3.58	3.45	2.85	2.73
6	2.98	—	3.76	3.63	3.05	2.95
7	3.03	—	3.90	3.77	3.19	3.09
8	3.04	—	3.82	3.69	3.17	3.05
9	3.04	—	3.93	3.79	3.25	3.12
10	3.13	—	4.04	3.91	3.32	3.17

An additional atom capped to pentagonal bipyramid of  $\text{Ge}_7$  yields the lowest energy structure for  $\text{Ge}_8$ . This structure is more stable over the bicapped octahedron by 0.08 eV. Both of these two structures are found for  $\text{Ge}_8$  in Car-Parrinello simulation, while bicapped octahedron is lower in energy by 0.03 eV<sup>28</sup>.

A bicapped pentagonal bipyramid is found for  $\text{Ge}_9$ . It is more stable than a capped distorted square antiprism by 0.06 eV. The current ground state structure has been found in Car-Parrinello simulation for  $\text{Ge}_9$ <sup>28</sup> but it is 0.08 eV higher than the capped square antiprism structure.

For  $\text{Ge}_{10}$ , the tetracapped trigonal prism ( $\text{C}_{3v}$ ) is found to be most stable and 0.16 eV lower than the bicapped square antiprism ( $\text{D}_{4d}$ ). This ground state structure is consistent with previous LDA results<sup>26,28</sup>.

In Table IV, we compare the binding energy per atom  $E_b/n$  for  $\text{Ge}_n$  ( $n = 2 - 10$ ) with the other theoretical and available experimental results. Due to the local density approximation, LDA calculation<sup>26,28</sup> has systematically overestimated the cluster binding energies. The more accurate binding energies for small germanium clusters up to five atoms has been provided by a more sophisticated G2(MP2) computation<sup>21</sup>. Although all the empirical parameters in our NTB model are fitted from dimer and bulk solid and there is no bond counting correction included, the experimental cohesive energies are fairly well reproduced by our calculation. Typical discrepancy between our calculation and experiment is less than 0.1 eV for those clusters. The successful description of binding energy within the present size range further demonstrates the transferability of the nonorthogonal tight-binding approach. In Table IV, we have also included the binding energies from Menon's NTB model for  $\text{Ge}_n$  clusters<sup>13</sup>. Although the geometries of  $\text{Ge}_n$  found in their work is almost the same as our results, the binding energies of  $\text{Ge}_n$  starting from  $\text{Ge}_5$  in Ref.13 are about  $0.10 \sim 0.2$  eV higher than our results and experimental values.

In summary, a nonorthogonal tight-binding model for germanium has been developed in this work. The transferability of the model is tested by various of bulk phases. The agreements between NTB model and *ab initio* results for bulk solids and small clusters are

satisfactory. For most  $\text{Ge}_n$  cluster with  $n = 3$  to 10, the ground state geometries from tight-binding model coincide with those from *ab initio* calculation. The only exceptional cases are  $\text{Ge}_8$  and  $\text{Ge}_9$ , in which the *ab initio* metastable isomers are predicted as ground states by NTB scheme. However, the energy difference between the ground state configuration and the isomer is less than 0.01 eV/atom and within the accuracy of tight-binding approach. Therefore, the NTB model developed in this work can be applied to explore the configuration space of larger germanium clusters with  $n > 10$ , for which a global minimization at the *ab initio* level is significantly more expensive. Our further studies shall include a genetic algorithm for sampling the phase space and finding possible low energy structural isomers of germanium clusters. Thus, first principle structural optimization can be performed on these local minima structures. On the other hand, this model will be also employed to simulate the thermodynamic properties such as melting and growth process of germanium cluster, which require a long time scale in TBMD simulation.

This work is partially supported by the U.S. Army Research Office (Grant DAAG55-98-1-0298) and the National Natural Science Foundation of China. The author (J.Zhao) are deeply grateful to Prof.E.Tosatti, Dr.J.Kohanoff, Dr.A.Buldum, and Prof.J.P.Lu for discussions.

\*Corresponding author: zhaoj@physics.unc.edu

## REFERENCES

<sup>1</sup> C.Z.Wang, K.M.Ho, in *Advances in Chemical Physics*, Vol.XCIII, p.651, Edited by I.Prigogine, S.A.Rice, (John Wiley & Sons, Inc., New York, 1996).

<sup>2</sup> C.M.Goringe, D.R.Bowler, E.Herhandez, Rep.Prog.Phys.**60**, 1447(1997).

<sup>3</sup> Computational Material Science, Vol 12, No.3 (1998): special issue on tight-binding molecular dynamics, Edited by L. Colombo.

<sup>4</sup> M.P.Aleen, D.J.Tidesley, *Computer Simulation of Liquids*, (Clarendon Press, Oxford, 1987).

<sup>5</sup> M.C.Payne, M.T.Teter, D.C.Allen, T.A.Arias, J.D.Joannopoulos, Rev.Mod.Phys.**64**, 1045(1992).

<sup>6</sup> G.Galli, A.Pasquarello, in *Computational Simulation in Chemical Physics*, edited by M.P.Allen and D.J.Tildesley, (Kluwer, Academic Publisher, 1993), p.261.

<sup>7</sup> L.Goodwin, A.J.Skinner, D.G.Pettifor, Europhys.Lett.**9**, 701(1989).

<sup>8</sup> C.H.Cu, C.Z.Wang, C.T.Chan, K.M.Ho, J.Phys.Condens.Matter **4**, 6047(1992).

<sup>9</sup> I.Kwon, R.Biswas, C.Z.Wang, K.M.Ho, C.M.Soukolis, Phys.Rev.B**49**, 7242(1994).

<sup>10</sup> M.Menon, K.R.Subbaswamy, M.Sawtarie, Phys.Rev.B**48**, 8398(1993).

<sup>11</sup> M.Menon, K.R.Subbaswamy, Phys.Rev.B**50**, 11577(1994).

<sup>12</sup> M.Menon, K.R.Subbaswamy, Phys.Rev.B**55**, 9231(1997).

<sup>13</sup> M.Menon, J.Phys.Condens.Matter.**10**, 10991(1998).

<sup>14</sup> M.van Schilfgaarde, W.A.Harrison, Phys.Rev.B**33**, 2653(1986).

<sup>15</sup> J.C.Slater, G.F.Koster, Phys.Rev.**94**, 1498(1954).

<sup>16</sup> C.Kittle, *Introduction to Solid State Physics*, (John Wiley & Sons, New York, 1986).

<sup>17</sup> D.A.Papaconstantopoulos, *Handbook of the Band Structure of Elemental Solids*, (Plenum Press, New York, 1986).

<sup>18</sup> W.A.Harrison, *Electronic Structure and the Properties of Solids*, (Freeman, San Francisco, 1980).

<sup>19</sup> J.E.Kingcade, U.V.Choudary, K.A.Gingerich, Inorg.Chem.**18**, 3094(1979); A.Kant, B.H.Strauss, J.Chem.Phys.**45**, 822(1966).

<sup>20</sup> C.C.Arnold, C.Xu, G.R.Burton, D.M.Neumark, J.Chem.Phys.**102**, 6982(1995).

<sup>21</sup> P.W.Deutsch, L.A.Curtiss, J.P.Blaudeau, Chem.Phys.Lett.**270**, 413(1997).

<sup>22</sup> H.B.Huntington, in *Solid State Physics*, Vol.7, p.214, ed. by F.Seitz and D.Turnbull, (Academic Press, New York, 1958).

<sup>23</sup> J.J.Zhao, A.Buldu, J.P.Lu, C.Y.Fong, Phys.Rev.B**60**, 14177(1999).

<sup>24</sup> D.Dai, K.Sumathi, K.Ralasubramanian, Chem.Phys.Lett.**193**, 251(1992); D.Dai, K.Balasubramanian, J.Chem.Phys.**96**, 8345(1992); D.Dai, K.Balasubramanian, J.Chem.Phys.**105**, 5901(1996).

<sup>25</sup> J.R.Chelikowsky, S.Ogut, X.Jing, K.Wu, A.Stathopoulos, Y.Saad, Mater.Res.Soc.Symp.Proc.**408**, 19(1996).

<sup>26</sup> S.Ogut, J.R.Chelikowsky, Phys.Rev.B**55**, 4914(1997).

<sup>27</sup> E.F.Archibong and A.St-Amant, J.Chem.Phys.**109**, 961(1998).

<sup>28</sup> Z.Y.Lu, C.Z.Wang, K.M.Ho, Phys.Rev.B**61**, 2329(2000).

<sup>29</sup> K.Raghavachari, C.M.Rohlfing, J.Chem.Phys.**89**, 2219(1988).

<sup>30</sup> J.M.Hunter, J.L.Fye, M.F.Jarrold, Phys.Rev.Lett.**73**, 2063(1993).